Radiation Protection Dosimetry (2008), Vol. 132, No. 3, pp. 277–282
Advance Access publication 28 October 2008
doi:10.1093/rpd/ncn280

DOSE MEASUREMENTS AROUND SPALLATION NEUTRON SOURCES

M. Fragopoulou[1,*], S. Stoulos[1], M. Manolopoulou[1], M. Krivopustov[2] and M. Zamani[1]
[1]Physics Department, Aristotle University of Thessaloniki, Thessaloniki 54 124, Greece
[2]Joint Institute for Nuclear Research, 141980 Dubna, Russian Federation

Received April 23 2008, revised August 29 2008, accepted September 24 2008

Neutron dose measurements and calculations around spallation sources appear to be of great importance in shielding research. Two spallation sources were irradiated by high-energy proton beams delivered by the Nuclotron accelerator (JINR), Dubna. Neutrons produced by the spallation sources were measured by using solid-state nuclear track detectors. In addition, neutron dose was calculated after polyethylene and concrete, using a phenomenological model based on empirical relations applied in high-energy physics. The study provides an analytical and experimental neutron benchmark analysis using the transmission factor and a comparison between the experimental results and calculations.

INTRODUCTION

Spallation is an efficient reaction for releasing neutrons from nuclei. In order to sustain spallation reactions, an energetic beam of light particles has to be supplied into a heavy target. However, during the spallation process, neutrons, protons, photons as well as other light particles are emitted from the target nucleus. Due to the high level of radiation generated, a spallation facility is required for transmutation studies. Therefore, it is necessary for an appropriate shielding surrounding the source to be constructed for radiation protection purposes. Several experiments were performed in order to study the neutron shielding in nuclear reactors[1–3], as well as in high-energy accelerators[4,5]. Radiation effects in a spallation environment are different from that commonly encountered in a reactor or accelerator because spallation sources can generate higher neutron densities and harder spectra than the nuclear reactors[6]. Hence, calculations and measurements of the neutron dose around spallation sources are of great importance.

The neutron spectrum produced by a spallation source has been thoroughly investigated during the last decades, especially at low energy region $E_n <$ 5 MeV[7,8]. Such experiments have also been performed in Dubna using a large cylindrical Pb target surrounded by a paraffin moderator or an U-blanket[9,10]. However, dose measurements after shielding are rarely presented in the literature. The cost of the radiation shielding contributes to a considerable part of the total financial cost of the spallation source, since massive shields for high-energy neutrons, having strong penetrability, are required.

*Corresponding author: fragom@auth.gr

The most common materials used as shielding materials are: concrete, iron, polyethylene, paraffin and graphite. In the present research, only polyethylene and concrete were studied as shielding materials.

In radiation shielding research, non-charged particles, such as photons and neutrons, are the main radiation to be considered. In order to design the optimal shielding, calculations were performed by taking into account mainly the neutron contribution. The criterion for the appropriate shielding is a dose rate lower than 1 μSv h^{-1}[11–15] and inexpensive construction materials. In the current study, calculations were performed using the phenomenological model based on empirical relations from high-energy physics. In addition, the neutron doses after shielding materials were measured on two different spallation sources. Analytical and experimental benchmark analysis has been performed using the neutron transmission factor.

EXPERIMENTAL

This work deals with the neutron dose produced by two different spallation neutron sources. In the first spallation source, the Gamma-2 set-up, a cylindrical Pb target was covered with a paraffin moderator and irradiated by 0.65 and 1 GeV protons. The Pb target was cylindrical with 8 cm diameter and 20 cm length and the paraffin moderator that surrounded the target was also cylindrical with 6 cm thickness. The paraffin was opened from the beam side (Figure 1a). The specific spallation source was intended to moderate the hard neutron spectrum produced by the Pb target. In the second set-up, ‘Energy plus Transmutation’ (‘E + T’), a cylindrical Pb target was covered with four sections of natural uranium blanket and was irradiated by protons with energy from 0.7 up to 2 GeV (Figure 1b). The construction of this spallation source was done in order to achieve a higher multiplication factor when compared with the paraffin moderator and harder neutron spectrum. For radiation protection reasons, 26 cm of polyethylene surrounded the ('E + T') spallation source. In addition, a Cd foil of 1 mm in thickness was covered on both sides of polyethylene to prevent U-blanket irradiation from low-energy backscattered neutrons. Both spallation sources had a simple geometry in order to be used for further benchmark analysis.

In both experiments, the experimental hall was shielded by 1 m concrete (Figure 1c). The spallation sources were positioned in the middle of the experimental hall, ~3 m from the concrete. The neutron spallation sources were irradiated in the Nuclotron accelerator, at the Laboratory of High Energy of the Joint Institute for Nuclear Research (JINR), Dubna.

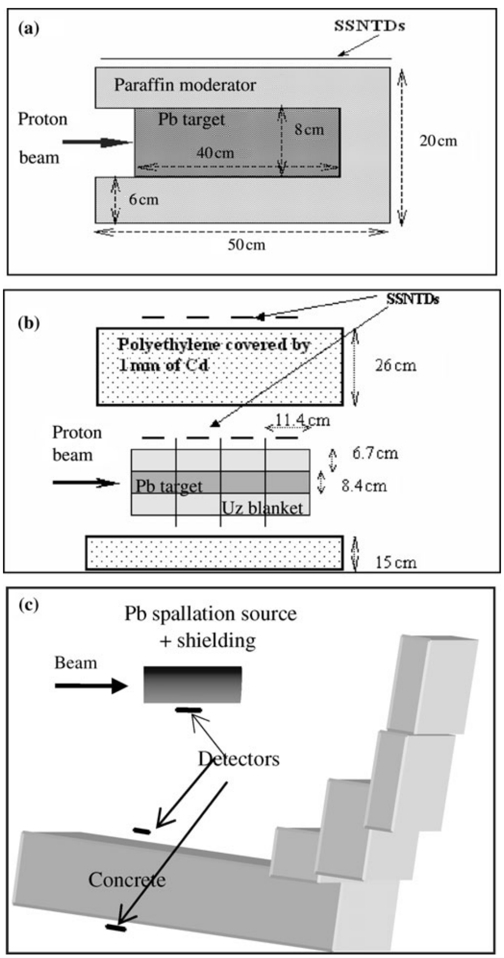

Figure 1. The spallation sources studied in the present work: (**a**) 'Gamma-2' (**b**) 'Energy plus Transmutation' assembly and (**c**) a diagram illustrating the concrete shielding and the location of the detectors.

The neutron fluence produced by both spallation sources, as well as the neutron fluence escaping from the shielding materials, was measured. The measurements were performed using solid-state nuclear track detectors (SSNTDs). Each set of SSNTDs contained polly allyl diglycol carbonate (PADC) foils (Pershore Mouldings standard grade, PM355), acting as a particle detector (Figure 2). The foils, 250 μm in thickness, were placed parallel to the target axis after the shielding materials. One part of the detector was in contact with a neutron converter (Kodak LR115 type 2B, containing $Li_2B_4O_7$). That part of the detector provided information about the total neutron fluence, by detecting the alpha particles' emitted via $^{10}B(n, \alpha)^7Li$ and $^6Li(n, \alpha)^3H$ reactions. Another part of the detector was in contact with the converter and was covered on both sides with 1 mm Cd foils, detecting likewise resonance up to fast neutrons. The thermal–epithermal neutron component (up to ~1 eV) was calculated by subtracting the measured track density of the Cd-covered from the Cd-uncovered region of the detector. Fast neutrons were also determined by proton recoil tracks on the detector itself (neutron elastic scattering on H of the detector)[16]. The neutron energy region detected by proton recoils was between 0.3 and 3 MeV due to limitations in the proton registration efficiency[17].

The dosemeters were calibrated in the frame of EURADOS actions for neutron dosimetry[16,18]. The calibration track number to neutron ambient dose equivalent was performed by irradiations with monoenergetic neutrons from 144 keV up to 15.3 MeV. Linearity, energy and angular response were studied. Moreover, calibrations for thermal (0.025 eV) and 24 keV neutrons were also performed. Because of the absence of experimental data, the response in the energy range between thermal and

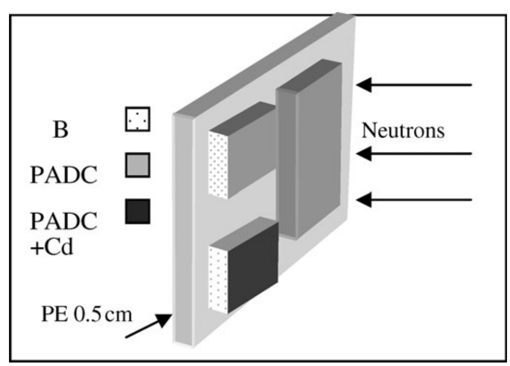

Figure 2. Design of the SSNTDs arrangement for neutron measurements.

24 keV neutrons could be expressed by a $1/E$ function. The conversion of track number to neutron ambient dose equivalent was made using conversion coefficients derived from the calibration[16,19], for each neutron energy region.

RESULTS AND DISCUSSION

In order to study neutron dose rates after the shielding, the neutron spectrum produced by the spallation sources was calculated after the shielding by using the Moyer model. The Moyer model is a point kernel method, which is based on the exponential attenuation of neutrons by a thick shield, considering that neutrons have reached the equilibrium state[20]. A comparison between the calculated and measured doses was also performed.

Experimental results

An efficient shielding attenuates high-radiation intensities, such as those produced by a spallation source, resulting in acceptable dose rate levels after the shielding. In order to select an appropriate shielding to surround a spallation source, the neutron dose produced by the source must be determined. Therefore, SSNTDs were placed along both the spallation sources, parallel to the target axis above the paraffin and the U-blanket. Thermal–epithermal and intermediate–fast neutrons were measured[21,22]. The neutron spatial distribution along the target axis for both spallation sources was found to be similar across all proton beam energies. For the conversion of neutron fluence to ambient dose equivalent, the corresponding conversion coefficient neutrons to $H^*(10)$, to each neutron energy bin, was used[16,23,24]. The experimental results are summarised in Table 1. According to the findings, the neutron ambient dose equivalent increased with the beam energy. The main part of the dose is attributed to fast neutrons. In Table 1, uncertainties of each value resulted from track measurements and the conversion coefficients. In Tables 2 and 3, the uncertainties were almost the same.

The total neutron ambient dose equivalent measured at the U-blanket surface of the ‘E + T’ set-up was found to be higher than the corresponding one at the paraffin surface of the ‘Gamma-2’ set-up. For radiation protection purposes, a polyethylene shielding surrounded the ‘E + T’ source. SSNTDs were placed above the polyethylene moderator that covered the U-blanket[25] in the direction parallel to the target axis (Figure 1b). The polyethylene moderator reduced the neutron ambient dose equivalent measured at the U-blanket surface ~60 times for 0.7 GeV and 30 times for 2 GeV. The neutron spectrum produced by the ‘E + T’ set-up was calculated using MCNPX and DCM/DEM codes[26,27]. According to the Monte Carlo calculation of the neutron spectrum, in which all neutrons are taken into account (including neutrons above 3 MeV), the moderator diminishes the neutron dose ~100 times for 1 GeV proton beam. Fast neutrons produced the main part of the total dose after polyethylene (Table 2). The comparison of neutron ambient dose equivalents produced by the two sources showed that the Gamma-2 set-up gave lower doses than the ‘E + T’ set-up. However, after the polyethylene moderator, the ‘E + T’ set-up produced smaller doses than the Gamma-2 set-up. The neutron ambient dose equivalent after experimental hall shielding, composed of iron-enriched concrete (heavy concrete), is the most important factor for radiation protection. The results

Table 1. The neutron ambient dose equivalent (Sv) measurements on the ‘Gamma-2’ and U-blanket surfaces during the total irradiation.

Proton energy (GeV)	Thermal–epithermal (Sv)	Intermediate–fast (Sv)
Gamma-2 surface		
0.65	0.22 ± 0.02	5 ± 1.5
1	0.61 ± 0.03	8 ± 3
U-blanket surface		
0.7	0.11 ± 0.01	12 ± 1.5
1	0.16 ± 0.03	17 ± 4
1.5	0.25 ± 0.04	28 ± 3
2	0.32 ± 0.09	38 ± 4

Table 2. Neutron dose measurements (mSv), during the total irradiation, after 26 cm polyethylene and 1 mm Cd of ‘E + T’ spallation source.

Proton energy (GeV)	Thermal–epithermal (mSv)	Intermediate–fast (mSv)
0.7	2.86 ± 0.26	204 ± 25
1	4.16 ± 0.78	289 ± 68
1.5	21.5 ± 3.4	812 ± 87
2	41.6 ± 11.7	1370 ± 144

Table 3. Neutron dose measurements, during the total irradiation, after the concrete for Gamma-2 and ‘E + T’ set-ups.

Proton energy (GeV)	Thermal–epithermal (μSv)	Intermediate–fast (μSv)
‘Gamma-2’ spallation source		
0.65	298 ± 46.5	<50
1	411 ± 114	<50
‘E + T’ spallation source		
1.5 GeV	<1.5	<50

after the concrete shielding are summarised in Table 3. As presented in the table, the neutron ambient dose equivalent after the concrete for the 'Gamma-2' set-up was higher than those for the 'E + T' set-up. The main part of the neutron ambient dose equivalent for the 'Gamma-2' set-up was produced from thermal–epithermal neutrons. In 'E + T', the neutron ambient dose equivalent derives from intermediate–fast neutrons and have the tendency to meet radiation protection standards. The total neutron ambient dose equivalent for the case of the Gamma-2 set-up remained higher than radiation protection standards. In the case of the 'E + T' set-up, the level of neutron ambient dose equivalent cannot be compared with radiation protection standards because it is less than the lower detection limit, which is 5×10^2 tracks cm^{-2}. According to dose calibrations of the detector, this track number corresponds to 1.5 μSv for thermal neutrons and ~50 μSv for fast neutrons.

Calculations

An analytical calculation of the neutron ambient dose was made for both spallation sources. Two assumptions are often made in shielding calculations for thin target sources. The first assumption is that the source can be approximated by a point source. For this assumption, the source must be localised in a geometrical volume that is small compared with the other dimensions of the shielding. The second assumption is that the dose D, as a function of the source position, could be described in terms of the relative coordinates of the point source with the point of interest and that there is no contribution from any other secondary sources. This assumption represents a pure point source/line-of-sight model. Such a model is directly applicable to the shielding of low-energy proton accelerators and has been extended to proton energies in the GeV range by Moyer. In the current study, the Moyer model was applied in low-energy neutrons, in order to be used for dose calculations after the shielding surrounding thick targets as in the case of spallation sources. The point kernel method, known as the Moyer model, is based on exponential attenuation of neutron dose equivalent for neutrons, when they reach the equilibrium state after thick shields[20], using a single built-up factor and an attenuation length. According to this model, the ambient dose equivalent at the point of interest can be estimated using the following phenomenological equation[28]:

$$H(x,\theta) = \frac{H_o(\theta)}{r^2}\exp\left(-\frac{x}{g(\theta)\lambda}\right) \qquad (1)$$

where $H_o(\theta)$ is taken as $H_o(90^\circ)$, representing the equivalent dose from the number of neutrons crossing at 90° the source surface. The calculation was made only for 90° because the maximum of the detector's efficiency is at 90° while in the intermediate angles between 90° and 0° it drops according to the law of $1/\cos^2\theta$, as it does for every flat detector. The variable r corresponds to the distance between the source and the point of interest, x the depth inside the shielding, $g(\theta)$ defined as $\sin\theta$ for lateral shielding and λ the interaction length. However, for lower energies, the interaction length depends on the neutron energy and the simple Moyer model is no longer applicable. In order to use the Moyer model for low-energy neutrons, the interaction length of neutrons has to be estimated for a shielding material in each neutron energy range. The interaction length of neutrons for each energy bin has been calculated using the relationship between the interaction length and the inelastic cross section[28]. Using the same relationship, the mean free path of neutrons can also be estimated. After the estimations of interaction length and the mean free path of neutrons for each neutron energy range, the neutron spectrum after the shielding can be calculated, taking into account the lethargy of neutrons in a shielding material, using Equation (1). In order to calculate the neutron spectrum after the shielding material, the neutron spectrum produced by the spallation sources was taken from the calculations made using the Monte Carlo DCM/DEM code[26]. In calculations, the statistical errors ranged between 3 and 6%[27]. The neutron ambient dose equivalent was estimated by taking into account the dose equivalent factor $H^*(10)$[23,24] for each energy point of the calculation. Shielding (or moderator) materials, such as polyethylene and concrete, were studied and the obtained results are presented in Table 4.

Comparison between measurements and calculations

Regarding the results presented in Tables 3 and 4, the calculation can satisfactorily describe the experimental results. For the comparison of the above calculations with the experimental results, the transmission factor of neutrons after the shielding was estimated. The transmission factor was defined as the ratio of the neutron ambient dose equivalent values with and without shield. The transmission

Table 4. Calculated neutron ambient dose equivalent after the shielding surrounded both spallation sources.

Proton energy (GeV)	Thermal–epithermal	Intermediate–fast
After concrete, 'Gamma-2' source		
1 GeV	375 μSv	20.1 μSv
After concrete, 'E + T' source		
1.5 GeV	1.26 μSv	26.1 μSv
After polyethylene, 'E + T' source		
1.5 GeV	34.3 mSv	880 mSv

Table 5. Transmission factor of neutrons (%).

Neutron energy range	Calculation	Measurement
After polyethylene, 'E + T' source		
Thermal–epithermal	8.4	8.6 ± 0.3
Intermediate–fast	2.6	2.9 ± 0.8
After concrete, 'Gamma-2' source		
Thermal–epithermal	0.25	0.18 ± 0.03

factor of neutrons after polyethylene for both thermal–epithermal and intermediate–fast neutrons is presented in Table 5. According to Table 5, the calculations converge to the experimental results. These analytical calculations based on the Moyer model indicate that this model can be applied to estimate the neutron dose after shielding. The differences observed between experiment and calculation can be attributed to the initial assumptions made for the application of the model, i.e. the spallation sources cannot be considered as a point source because they have significant dimensions.

CONCLUSION

The main objective of the present study was to determine experimentally and by calculation the ambient dose equivalent induced by neutrons produced by two different spallation sources, consisting of the Pb target. Table 1 shows that the 'E + T' set-up gave higher neutron doses compared with the Gamma-2 set-up for the same proton beam energies. This effect is due to the higher fast neutron production from the 'E + T' set-up compared with the spectrum corresponding to the Gamma-2 set-up. Gamma-2 spectrum contained more thermal–epithermal neutrons than the 'E + T' set-up, in which the thermal neutron contribution (thermal < 1 eV) is negligible, as confirmed experimentally. In a U-blanket surface, some thermal neutrons come from neutron back scattering in the polyethylene shielding and it was found to be of the order of 10^{-5} cm^{-2} per proton incident on the target.

The polyethylene shielding diminished the total neutron ambient dose equivalent of the 'E + T' set-up ~100 times. However, a part of those neutrons were shifted to the thermal–epithermal neutron range. Their contribution to the total neutron ambient dose equivalent after polyethylene was ~100 times lower than the fast neutron dose. From these neutrons, the ratio of intermediate–fast/thermal–epithermal is ~70 for 0.7 GeV and 30 for 2 GeV. In conclusion, the polyethylene shielding reduced the dose of the 'E + T' set-up below the one corresponding to the Gamma-2 set-up.

For both set-ups, after concrete the fast neutron component was below the detection limit of the PADC, which was 5×10^2 tracks per cm^2 for fast neutrons. The dose coming from thermal–epithermal neutrons was found to be higher for the Gamma-2 set-up than for the 'E + T' set-up. The comparison between the experimental results and calculations showed a good agreement (Table 5) for both thermal–epithermal and intermediate–fast neutrons. For fast neutrons, the same comparison after concrete was not feasible because their number is below the detection limit.

The agreement of experimental results with analytical calculations based on the Moyer model, demonstrates that the application of the model could be employed for low-energy neutrons without significant deviations. The results also indicated that the model applied for thin targets could be used for thick targets with large dimensions compared with a point source with a deviation of 3–30%. The large deviation is due to the small track number measured, which induces large experimental uncertainties.

In order to compare the ambient dose equivalent with radiation protection standards after concrete, the ambient dose equivalent has been converted to dose rates. For this estimation, the duration of the irradiations (to complete ~10^{13} beam protons) was taken into account. The total neutron ambient equivalent dose rate produced by both spallation sources was calculated by applying appropriate conversion factors to the data obtained using MCNPX and DCM/DEM codes. According to the last radiation protection recommendations of 2007, the effective dose limits in planned occupational exposure must be <20 mSv y^{-1}, averaged over defined periods of 5 y[14]. The commission has concluded that the existing dose limit recommended by ICRP60 continues to provide an appropriate level of protection[11]. For this research, the ambient dose equivalent was used instead of effective dose, taking into account that for the recommended effective dose limit the total tissue weighting factor was 1 ($\sum W_T = 1$). The tissue weighting factor for a uniform irradiation of a body can be taken as equal to one[11]. An additional constraint of 1 μSv h^{-1} neutron ambient dose equivalent for workers is an optimum lower limit. The total neutron ambient equivalent dose rate after concrete in the described experiments was found to be higher than the maximal allowed effective dose in personal dosimetry determined by ICRP[11–14]. For the Gamma-2 set-up, the dose rate is 37 μSv h^{-1} (34 μSv h^{-1} from thermal–epithermal and 2.5 μSv h^{-1} from fast neutrons) for proton beam of 1 GeV. For the 'E + T' set-up, 11 μSv h^{-1} were estimated (~0.5 μSv h^{-1} from thermal–epithermal and 10 μSv h^{-1} from fast neutrons) for 1.5 GeV protons. These findings suggest that an additional shielding has to be calculated for spallation sources. The most practical and cost-effective solution is to add iron (of ~40 cm) from the experimental hall side taking into account the neutron's calculations from Monte Carlo results.

ACKNOWLEDGEMENT

The authors are grateful to Professor A.I. Malakhov and the staff of the Laboratory of High Energies, JINR Dubna, for their continuous support. The authors would also like to express their special gratitude to Professor A.D. Kovalenko and the operators of the NUCLOTRON accelerator.

REFERENCES

1. Kenneth Shultis, J. and Faw, R. E. *Radiation shielding technology.* Health Phys. **88**, 297–322 (2005).
2. Nines, J. C. and Waker, A. J. *Multisphere spectrometry and analysis of TEPC and REM meter results around a heavy water moderated reactor.* Radiat. Prot. Dosim. **59**, 279–284 (1995).
3. Deboodi, P., Vermeersch, F., Vanhavere, F. and Minsart, G. *Neutron dosimetry at the reactor facility VENUS.* Radiat. Prot. Dosim. **70**, 187–192 (1997).
4. Moritz, L. E. *Review of proton accelerator shielding problems.* In: Proceedings of an AEN/NEA Specialists' Meeting on Shielding Aspects of Accelerators, Targets and Irradiation Facilities, SATIF. Vol. 6, Cyric, Sendai, Japan, 12–13 May 1997, pp. 93–106 (1997).
5. Stevenson, G. R. *Shielding high energy accelerators.* Radiat. Prot. Dosim. **96**, 359–371 (2001).
6. Bauer, G. S. *Physics and technology of spallation neutron sources.* Nucl. Instrum. Methods Phys. Res. A **463,** 505–543 (2001).
7. Letourneau, A. *et al. Neutron production in bombardments of thin and thick W, Hg, Pb targets by 0.4, 0.8, 1.2, 1.8 and 2.5 GeV protons.* Nucl. Instrum. Methods Phys. Res. B **170**, 299–322 (2000).
8. Leray, S. *et al. Spallation neutron production by 0.8, 1.2, and 1.6 GeV protons on various targets.* Phys. Rev. C **65**, 044621–044638 (2002).
9. Krivopustov, M. I. *et al.* First experiments with a large Uranium Blanket within the installation 'Energy plus transmutation' exposed to 1.5 GeV protons. Kerntechink **68**, 48–55 (2003).
10. Adam, J. *et al. Transmutation studies with GAMMA-2 setup using relativistic proton beams of the JINR Nuclotron.* Nucl. Instrum. Methods. Phys. Res. A **562**, 741–742 (2006).
11. ICRP 60. *1990 Recommendations of the International Commission on Radiological Protection*. Ann. ICRP. **21**(1–3) (1991b).
12. ICRP 68. *Dose coefficients for intakes of radionuclides by workers.* Ann. ICRP. **24**(4) (1994c).
13. ICRP 75. *General principles for the radiation protection of the workers.* Ann. ICRP. **27**(1) (1997a).
14. ICRP 103. *Recommendations of the International Commission on Radiological Protection*. Ann. ICRP. **37**(2–4) (2007).
15. Fasso, A. *et al. Intermediate energy nuclear data: models and codes.* In: Proceedings of a Specialists Meeting, Issy les Moulineaux (France), 30 May–1 June (Paris: OECD) p. 271 (1994).
16. Zamani, M., Sampsonidis, D. and Savvidis, E. *An individual neutron dosimeter with (n,α) and (n,p) converters.* Radiat. Meas. **26**, 87–92 (1996).
17. Harvey, J. R., Tanner, R. J., Alberts, W. G., Bartlett, D. T., Piesch, E. K. and Schraube, H. *The contribution of Eurados and Cendos to track etch neutron dosimetry: the current status in Europe.* Radiat. Prot. Dosim. **77**, 267–304 (1998).
18. Van Dijk, W. E., Bordy, J. M., Vanhavere, F., Wernli, C. and Zamani-Valasiadou, M. *A review of the properties of the dosimetric systems and the quality assurance programmes of 48 dosimetric services in the European Union and Switzerland.* Radiat. Prot. Dosim. **96**, 151–157 (2001).
19. Stoulos, S., Fragopoulou, M., Manolopoulou, M., Sosnin, A., Krivopustov, M., Westmeier, W., Brandt, R., Debeauvais, M. and Zamani, M. *Neutron measurements by passive methods in the Dubna transmutation assemblies.* Nucl. Instum. Methods Phys. Res. A **519,** 651–658 (2004).
20. Moyer, B. J. *Evaluation of shielding required for improved betaron.* Lawrence Berkeley Laboratory report UCRL-9769 (Berkeley Laboratory, U.S. Department of Energy National Laboratory, University of California) (1961).
21. Zamani, M., Fragopoulou, M., Manolopoulou, M., Stoulos, S., Spyrou, A., Debeauvais, M., Brandt, R., Westmeier, W., Krivopustov, M. and Sosnin, A. *Spallation neutron production in the new Dubna transmutation assembly.* Nucl. Instrum. Methods Phys. Res. A **508**, 454–459 (2003).
22. Fragopoulou, M. *et al. Spatial distribution of moderated neutrons along a Pb target irradiated by high energy protons.* Nucl. Instrum. Methods Phys. Res. A **560**, 571–576 (2006).
23. Shin, K. and Ishii, Y. *Build-up factor for medium energy neutrons up to 400 MeV.* Radiat. Prot. Dosim. **40**, 185–194 (1992).
24. ICRU Report 57. *Conversion coefficients for use in Radiological Protection against External Radiation*. ICRU Report 57 (1998).
25. Fragopoulou, M., Manolopoulou, M., Stoulos, S., Brandt, R., Westmeier, W., Krivopustov, M., Sosnin, A., Golovatyuk, S. and Zamani, M. *Shielding around spallation neutron sources.* J. Phys., Conf. Ser. **41**, 514 (2006).
26. Sosnin, A. *et al. Influence of different moderator materials on characteristics of neutron fluxes generated under irradiation of lead target with proton beams.* JINR E2, **258**, 1–9 (2002).
27. Hashemi-Nezhad, S. R., Zhuk, I., Kievets, M., Krivopustov, M. I., Sosnin, A. I., Westmeier, W. and Brandt, R. *Determination of natural uranium fission rate in fast spallation and fission neutron field: an experimental and Monte Carlo study.* Nucl. Instrum. Methods Phys. Res. A **591**, 517–529 (2008).
28. Sullivan, A. H. A. *Guide to Radiation and Radioactivity Levels near High Energy Particle Accelerators* (England: Nuclear Technology Publishing) (1992).